



## Magnetron sputtering synthesis silver and organic PEO nanocomposite

Qiang Chen<sup>a,\*</sup>, Meili Zhou<sup>a</sup>, Yabo Fu<sup>a</sup>, Jing Weng<sup>b</sup>, Yuefei Zhang<sup>a</sup>, Lei Yue<sup>a</sup>, Fenyan Xie<sup>a</sup>, Chunqing Huo<sup>a</sup>

<sup>a</sup> Laboratory of Plasma Physics and Materials, Beijing Institute of Graphic Communication, Beijing, 102600, China

<sup>b</sup> Capital Medical Univ., Beijing, 100069, China

### ARTICLE INFO

Available online 21 June 2008

#### PACS:

52. 75. Hn

52. 77. Fv

52. 80. Hc

52. 80.Wq

#### Keywords:

Magnetron sputtering

Ag/PEO-like

Nanocomposite

### ABSTRACT

A nanocomposite, silver nanoparticles embedded into polyethylene oxide (PEO) is synthesized by magnetron sputtering. The embedded silver in PEO matrix is confirmed by transmission electron microscopy (TEM) image, X-ray diffraction (XRD) pattern, and atomic force microscopy (AFM) analysis. By TEM image the sizes of silver nanoparticles are found to be tunable, and the silver crystallization is preferentially grown in facet of (111) by varying the plasma parameters, especially the working pressure. The crystal statue is evidenced by UV–visible spectra where the peak of plasmon absorption is located at ca. 400 nm. This characterization is very important for silver nanocomposite application as an antibacterial reagent based on previous antimicrobial results. By Fourier transform infrared spectroscopy (FTIR) the functional group of C–O–C in PEO films is depicted to be enough retained from the monomer in MS plasma.

© 2008 Published by Elsevier B.V.

### 1. Introduction

There is an increasing interest in plasma-deposited thin films that possess bacterial resistibility and non-fouling property, especially in medicine where medical device infection is associated with significant healthcare costs [1,2]. Different approaches for preventing microbial adhesion and inhibiting bacteria growth have been proposed [3]. Polyethylene oxide (PEO) or PEO-like polymer is well known for its non-fouling behavior against the adhesion of cells, bacteria, proteins and other ones [4,5]. Silver is known as one of the oldest antibacterial agents, where silver ions are thought to inhibit bacterial enzymes and bind to DNA [6,7]. But now nano-scale silvers seem to demonstrate a more efficient role than that by ions [8].

Then plasma-deposited nanocomposite Ag/PEO(-like) coatings are expected as promising candidates as bacterial resistant coatings because of the merging of the non-fouling property of PEO (-like) [4,5,9] with the antibacterial property of silver [10,11]. For the non-fouling character of plasma-deposited PEO (-like) films, it is necessary that the C–O–C functional group in the monomer structure is retained as much as possible in the plasma polymerization chains. So in general a low power continuous wave or a long pulse duty pulsed plasma is employed to achieve this strategy. For metal particles, especially nano-

scale metal, chemical vapor metallic organic, or magnetron sputtering (MS) process is employed. But for organic–metal nanocomposite, due to the toxicity of target there are no approaches being reported until now.

In this paper we present the fabrication of nanocomposite: Ag nanoparticle embedded in organic polymer PEO proposed by MS plasma, i.e. in a properly configured magnetron sputtering volatile organic monomer is fed and fragmented by Ar ions to form organic polymer, and nano-scale silver is sputtered from target by Ar ions embedded into organic composite and form silver-PEO nanocomposite simultaneously.

### 2. Experimental

Nanocomposites are prepared in the chamber, which are evacuated below  $3.0 \times 10^{-3}$  Pa before depositions are carried out. For PEO film polymerization, glycol dimethyl ether is utilized as a precursor feeding into MS plasma. Nano-scale silver particles are obtained by magnetron sputtering technology driven by direct current (DC) power where argon gas is fed through mass flow controller. The DC MS plasma power is multiplied by measured voltage and current. The *p*-silicon wafers used as substrates are cleaned ultrasonically with ethanol, acetone and deionized water in sequence before they are mounted on the sample holder. In the experiment all parameters are kept constant while the working pressure is investigated for Ag/PEO fabrication.

The chemical components of the plasma polymerization organic films are characterized by Fourier transform infrared spectroscopy

\* Corresponding author. Laboratory of Plasma Physics and Materials, Beijing Institute of Graphic Communication, Xinghua north Street, Daxing, 102600, Beijing, China. Tel.: +86 10 6026 1099; fax: +86 10 6026 1108.

E-mail address: [chenqiang@bigc.edu.cn](mailto:chenqiang@bigc.edu.cn) (Q. Chen).

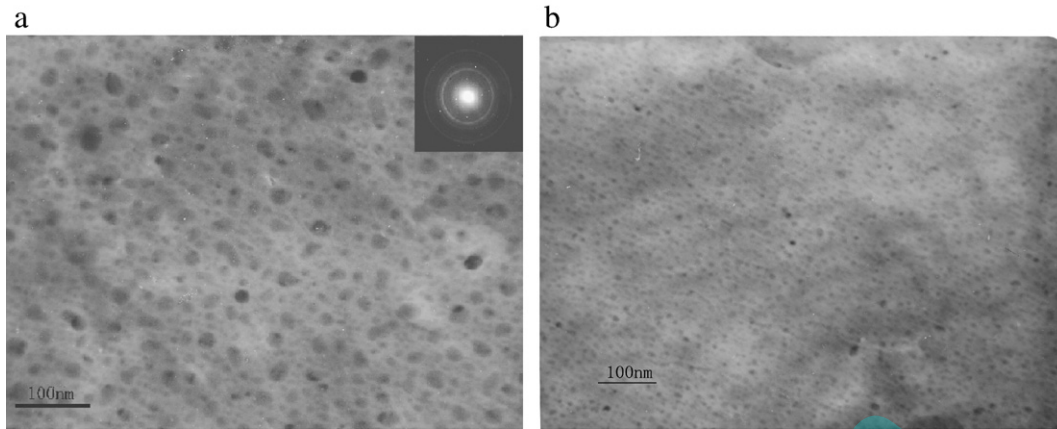


**Fig. 1.** The relationship of silver diameters embedded into PEO film by TEM image with working pressures. a—2.0 Pa; b—0.2 Pa (inset selected area electron diffraction (SAED) pattern, 10 sccm Ar, film thickness ca. 280 nm).

(FTIR) (Shimadzu, FTIR-8400). Atomic force microscopy (AFM) (CSPM3000, BenYuan) is also used in a tapping mode to analyze the surface morphology of films. The transmission electron microscopy (TEM) investigation for the concentration and diameter of Ag particles in nanocomposite is carried out by a Philips CM300 working at 300 kV and equipped with Super TWIN lenses. X-ray diffraction pattern (XRD) (MXP 18 AHF, X-ray diffractometer with monochromatized Cu K $\alpha$  radiation ( $\lambda = 1.54056 \text{ \AA}$ )) is employed to detect the particle size, and the silver crystal facets. And UV–visible (Perkin Elmer Lamda 900) is used to explore the silver diameter and status in nanocomposites.

### 3. Results and discussion

The TEM images in Fig. 1 exhibit that the diameters of silver nanoparticles sputtered by magnetron sputtering (MS) embedded simultaneously in the PEO polymer are tunable but depend on the working pressure. When the working pressure is in 0.2 Pa, the diameter of silver particles is in the range of 5–10 nm. The inset selected area electron diffraction (SAED) pattern clearly demonstrates that the particles are crystal in the matrix.

The X-ray diffraction (XRD) spectra for silver diffused PEO samples are shown in Fig. 2. The peaks at  $2\theta = 38.1^\circ$ ,  $44.2^\circ$ ,  $64.4^\circ$ , and  $77.3^\circ$  can be assigned to (111), (200), (220), and (311) crystalline planes of silver, respectively [12]. The strongest XRD peak at  $2\theta = 38.1^\circ$ , which corresponds to the (111) facet of silver, appeared at 0.2 Pa working

pressure depositing Ag/PEO sample. Comparing the intensity of  $I_{(111)}/I_{(200)}$ , one notes the low working pressure is preferred to forming silver (111) orientation in the polymer matrix.

By Scherer formula in Fig. 2, the calculated particle sizes of Ag are 22 nm, 11 nm, and 7 nm corresponding to 2.0 Pa, 1.0 Pa and 0.2 Pa working pressures, respectively. It is well consistent with diameters obtained in TEM image in Fig. 1.

According to the UV–visible spectra in Fig. 3, the absorption peaks due to the surface plasmon transverse resonance of Ag particle appeared around 400 nm but depend on the exposure times. The increase of deposition time induced a red-shifted peak from ca. 410 nm to 460 nm and maybe contributed to the silver size increase due to the aggregation of the nanoparticles with the excess exposure times [13].

One can clearly see from Fig. 4 of the AFM images that the films consisted of nanoparticle islands that are seemingly uniform in the surface. Comparing Fig. 4(a) and (b) the different diameters of the luminesced points in AFM images it is revealed that the diameter of clusters is greatly larger in Ag embedded composites than that only in pure PEO polymerization. It is evidenced that Ag nanoparticles are embedded into the polymer and deduced that the possible aggregation occurred to form Ag clusters when it is grown.

It is noted [8] that the silver nanoparticles in the range of 1–10 nm with preferential facet of (111) can very efficiently attach to the cell membrane surface and drastically disturb the bacteria's permeability

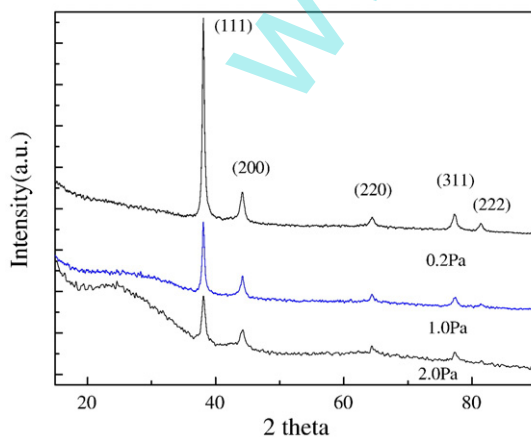


**Fig. 2.** XRD pattern of Ag particles embedded in PEO films of different working pressures (the same conditions as Fig. 1).

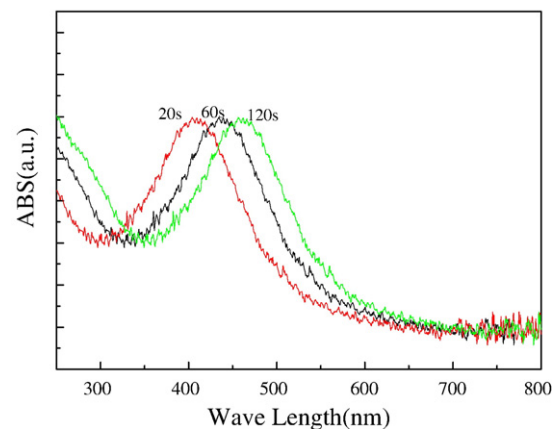


**Fig. 3.** The UV–visible absorption peaks of Ag particles are relevant to different deposition times (20 W, 10 sccm Ar, film thickness ca. 20 nm, 60 nm, and 120 nm, respectively).

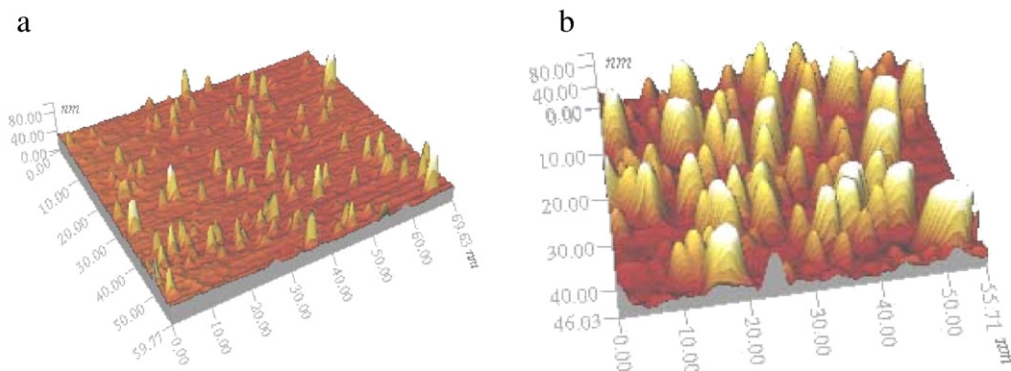


Fig. 4. AFM images of (a) pure PEO, and (b) Ag/PEO nanocomposite (film thickness ca. 300 nm).

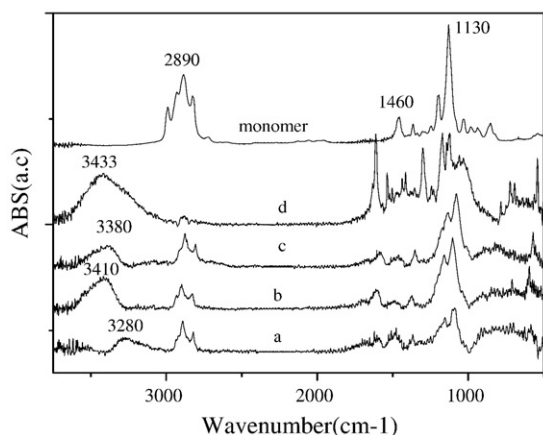


Fig. 5. The FTIR of Ag/PEO nanocomposites fabricated in magnetron sputtering by variation of the distance of target-to-substrate in a–90 mm; b–80 mm; c–70 mm; d–60 mm (film thickness ca. 300 nm).

and respiration functions. Our experimental results mean the approach here can offer a perfect character of tuned nanometallic particles and may be very efficient in the fabrication of diameter and facet controllable silver for antibacterial application.

FTIR spectra in Fig. 5 present the synthesized polymer components affected by the distance of substrate-to-target. It exhibit that, besides the stretching and vibration peaks assigned to  $-\text{CH}_2$  and  $-\text{CH}_3$  at 2950 to 2860  $\text{cm}^{-1}$  the spectra are deformed for MS plasma polymerization, peaks around 1130  $\text{cm}^{-1}$  assigned to C–O–C stretching bands are also widened and show a little bit red-shift to 1103  $\text{cm}^{-1}$  [14]. It is noticed that the C–O–C functional groups incorporating in polymer are enough retained by MS plasma when the distances are large. In 60 mm, however, one can see the C=O, C=C groups in ca. 1620  $\text{cm}^{-1}$  appeared, and  $-\text{CH}_2$  and  $-\text{CH}_3$  at 2950 to 2860  $\text{cm}^{-1}$  and 1460  $\text{cm}^{-1}$  nearly disappeared in the film due to the high Ar ion energy that fragmentize the main chain. The extra peak around 3400  $\text{cm}^{-1}$  assigned to  $-\text{OH}$  stretching that appeared in all MS films is suspected to be the post-reaction from the environment.

#### 4. Conclusions

In this work, Ag/PEO nanocomposites are deposited in an appropriately configured magnetron sputtering, where the silver sputtered from target and the PEO polymer polymerized take place simultaneously in MS plasma. TEM reveals that the preferred facet of (111) silver embedded uniformly in nanocomposite within tunable diameters can be prepared in this plasma source by changing the plasma working pressure. FTIR spectra reveal that the functional group C–O–C can be enough retained in the coating but depending on the distance of target-to-substrate.

#### Acknowledgements

This work is supported by NSFC (No.10475010, 10775017), the Beijing Key Scientific Research Foundation for Returned overseas, and PHR (IHLB) as well as KF060201.

#### References

- [1] P.T. Naylor, Clin. Orthop. Relat. Res. 261 (1990) 126.
- [2] T.L. Lin, F.M. Lu, M.S.A. Sheu, Med. Device Technol. 89 (2001) 11.
- [3] F. Furno, K.S. Morley, B. Wong, B.L. Sharp, P.L. Arnold, S.M. Howdle, R. Bayston, P.D. Brown, P.D. Winship, H. Reid, J. Antimicrob. Chemother. 54 (2004) 1019.
- [4] K.L. Prime, G.M. Whitesides, J. Am. Chem. Soc. 115 (1993) 10714.
- [5] E.E. Johnston, B.D. Ratner, J.D. Bryers, in: R. d'Agostino, P. Favia, F. Fracassi (Eds.), Plasma-Processing of Polymers, NATO ASI Series, E: Appl. Sci., vol. 346, Kluwer Acad. Publ., 1997, p. 123.
- [6] R.B. Thurman, C.P. Gerba, CRC Crit. Rev. Environ. Control 18 (1989) 295.
- [7] P.D. Bragg, D.J. Rainnie, Can. J. Microbiol. 20 (1974) 883.
- [8] Jose R. Morones, Jose L. Elechiguerra, A. Camacho, K. Holt, Juan B. Kouri, Jose T. Ramirez, M. Jose Yacaman, Nanotechnology 16 (2005) 2346.
- [9] G.P. Lopez, B.D. Ratner, C.D. Tidwell, C.L. Haycox, R. Rapoza, T.A. Horbett, J. Biomed. Mater. Res. 26 (1992) 415.
- [10] A. Oloffs, C. Grosse-Siestrup, S. Bisson, M. Rinck, R. Rudolph, U. Gross, Biomaterials 15 (1994) 753.
- [11] J.M. Schierholz, L.J. Lucas, A. Rump, G. Pulverer, Hosp. J. Interface 40 (1998) 257.
- [12] C.P. Lungu, K. Iwasaki, K. Kishi, M. Yamamoto, R. Tanaka, Vacuum 76 (2004) 119.
- [13] Y. Gao, P. Jiang, L. Song, L. Liu, X. Yan, Z.h. Zhou, D. Liu, J. Wang, H. Yuan, Z. Zhang, X. Zhao, X. Dou, W. Zhou, G. Wang, S. Xie, J. Phys., D, Appl. Phys. 38 (2005) 1061.
- [14] W.T. Wu, Y. Wang, L. Shi, Q. Zhu, W. Pang, G. Xu, F. Lu, Nanotechnology 16 (2005) 3017.